Zheying Guo
Mechanics of Soft Biological Systems Laboratory,
Department of Biomedical Engineering and Mechanics,
Virginia Tech,
330 Kelly Hall,
Blacksburg, VA 24061
e-mail: guozhy@vt.edu

Joseph W. Freeman
Musculoskeletal Tissue Regeneration Laboratory,
Department of Biomedical Engineering,
Rutgers University,
599 Taylor Road,
Piscataway, NJ 08854
e-mail: jfreemn@rci.rutgers.edu

Jennifer G. Barrett
Marion duPont Scott Equine Medical Center,
Department of Large Animal Clinical Sciences,
Virginia-Maryland Regional College of Veterinary Medicine,
Virginia Tech,
P.O. Box 1938,
Leesburg, VA 20176
e-mail: jgbarret@vt.edu

Raffaella De Vita
Mechanics of Soft Biological Systems Laboratory,
Department of Biomedical Engineering and Mechanics,
Virginia Tech,
330 Kelly Hall,
Blacksburg, VA 24061
e-mail: devita@vt.edu

Quantification of Strain Induced Damage in Medial Collateral Ligaments

In the past years, there have been several experimental studies that aimed at quantifying the material properties of articular ligaments such as tangent modulus, tensile strength, and ultimate strain. Little has been done to describe their response to mechanical stimuli that lead to damage. The purpose of this experimental study was to characterize strain-induced damage in medial collateral ligaments (MCLs). Displacement-controlled tensile tests were performed on 30 MCLs harvested from Sprague Dawley rats. Each ligament was monotonically pulled to several increasing levels of displacement until complete failure occurred. The stress–strain data collected from the mechanical tests were analyzed to determine the onset of damage and its evolution. Unrecoverable changes such as increase in ligament's elongation at preload and decrease in the tangent modulus of the linear region of the stress–strain curves indicated the occurrence of damage. Interestingly, these changes were found to appear at two significantly different threshold strains ($P < 0.05$). The mean threshold strain that determined the increase in ligament's elongation at preload was found to be 2.84% (standard deviation (SD) = 1.29%) and the mean threshold strain that caused the decrease in the tangent modulus of the linear region was computed to be 5.51% (SD = 2.10%), respectively. The findings of this study suggest that the damage mechanisms associated with the increase in ligament's elongation at preload and decrease in the tangent modulus of the linear region in the stress–strain curves in MCLs are likely different. [DOI: 10.1115/1.4030532]

1 Introduction

Sprains of knee ligaments are among the most common orthopedic injuries. They often occur when the ligaments are subjected to loads and deformations that are below their ultimate capacity but above some damage thresholds. While many investigators in biomechanics have focused on characterizing the ultimate loads and deformations of knee ligaments, little has been done to determine their mechanical damage thresholds. This is, perhaps, due to the lack of standardized methods in biomechanics for defining and measuring damage in collagenous tissues. Identifying and quantifying damage in ligaments is, however, crucial for the development of replacement grafts, bracing devices, and safe stretching routines. Replacement grafts must sustain the in vivo loads or deformations of native ligaments in order perform their function, without being damaged. Bracing devices must provide protection to the sprained ligaments during healing, and they must limit loads or deformations that lead to further damage. Finally, stretching routines for athletes must be carefully modulated to avoid the occurrence of ligament sprains during sport activities. For these reasons, new standardized methods are necessary to detect and evaluate loads and deformations that induce damage (not complete rupture) in ligaments.

Over the past few years, several studies have been carried out on different types of collagenous tissues to investigate damage through fatigue experiments [1–8]. In these studies, different damage parameters were defined in order to quantify the unrecoverable changes in the stress–strain or load–deformation curve of each fatigue cycle. In an earlier study by Wang et al. [6] on tendons, the decrease in cyclic peak stress was employed to detect fatigue damage. Similarly, King et al. [2] and Pollock et al. [3] used the decrease in cyclic peak load over the testing period as damage indicator in ligaments. Fatigue damage in ligaments and tendons was detected by estimating the decrease in stiffness [6], dynamic tensile modulus [4], secant modulus [7,8], or tangent modulus of the linear region [5] at each fatigue cycle. The reduction in stiffness/modulus measured as the number of fatigue cycles increased during testing was used as fatigue damage parameter. Moreover, the increase in ligament's length [3] or the clamp-to-clamp strain [1], and the elongation of the toe region [2,7], reported as the number of fatigue cycles increased, were also measured to study the damage evolution process. In the above cited studies, the damage on ligaments and tendons was, however, cumulative being produced by fatigue cycles.

There are a few studies that focus on determining damage in knee ligaments induced by monotonic tensile tests [9–11]. Monotonic tensile testing emulates the mechanical stimuli that produce sprains better than fatigue testing. Clinically, knee ligaments are often damaged after being loaded or deformed above some damage thresholds during single traumatic events. Panjabi et al. [9] conducted monotonic tensile tests on rabbit anterior cruciate ligaments (ACLs) at high (~1 m/s) and low (~1 mm/s) deformation rates. In their studies, each ligament was pulled to a subfailure

Manuscript received August 23, 2014; final manuscript received April 4, 2015; published online June 3, 2015. Assoc. Editor: David Corr.

deformation defined as 80% of the failure deformation. This failure deformation was computed from the paired contralateral ligament. The subfailure deformation produced an elongation of the load–deformation curve that was quantified by comparing the deformation of each pair of ACLs at different load levels. It also produced a change in stiffness computed at 50% of the failure load. Panjabi et al. [12] also compared the effect of a single subfailure stretch and a series of incremental subfailure stretches that ended at the same stretch value on the mechanical behavior of rabbit ACLs. They observed no significant difference in the load–deformation curves and viscoelastic properties of two groups of ligaments that were tested with the two different damage stretching protocols (single subfailure stretch and incremental subfailure stretches).

Damage thresholds were determined by Provenzano et al. [11] in rat MCLs by applying different subfailure stretches to different specimens, with each specimen receiving a single subfailure stretch. The unrecoverable increase in the preload length of the ligament subjected to a subfailure stretch was defined as structural damage. The structural damage data from different experiments performed by imposing different subfailure stretches on MCLs were calculated and fit to a linear model to obtain a strain of 5.14% that indicated the onset of damage.

In this study, the damage evolution process in rat MCLs was investigated by performing displacement-controlled tensile tests. The ligaments were subjected to monotonically increasing displacements. The unrecoverable changes in stress–strain curves were quantified and correlated with the strain corresponding to the applied incremental displacements. The proposed experimental protocol could provide a more accurate evaluation of strain-based damage thresholds for ligaments when compared to other protocols. Indeed, the damage thresholds were computed for each specimen and were not extrapolated from results obtained by testing different samples to different subfailure strains [11]. The evaluation of damage did not rely on the assumption of biomechanical symmetry of paired knee ligaments used in previous studies [9,10] and, hence, required the sacrifice of fewer animals. The outcome of this study may help the fields of orthopedics, sports medicine, and athletic training. For example, knowledge about strain-based damage thresholds for ligaments could be used together with current elastography techniques to prevent and treat sprains and other injuries caused by mechanical stimuli.

2 Materials and Methods

This study was conducted in accordance with applicable laws, regulations, guidelines, and policies (i.e., the U.S. Animal Welfare Act, Public Health Service Policy, U.S. Government Principles, and the Guide for the Care and Use of Laboratory Animals). All procedures were conducted with approval of the Institutional Animal Care and Use Committee at Virginia Tech. Sixteen Sprague Dawley male rats were purchased from Harlan Laboratories (Frederick, MD). The mean age of the rats was 84 days (SD = 3 days) and the mean body weight was 342 g (SD = 15 g). These rats are considered to be adult [13]. They were euthanized with 4 ml of Beuthanasia D solution (1560 mg pentobarbital sodium, 200 mg phenytoin sodium) by intraperitoneal injection. Immediately postmortem, the femur–MCL–tibia complexes (FMTCs) were carefully dissected from the hind limbs, wrapped in gauze moistened with phosphate buffered saline solution, sealed in plastic, and stored frozen (− 20 °C). Two FMTCs were damaged during dissection and, hence, were excluded from the study.

Before mechanical testing, the FMTCs were thawed at room temperature. The soft tissues around the knee joints were removed to expose the MCLs, while keeping them hydrated by constantly spraying phosphate buffered saline solution on their surface. Black ink was then sprayed on the surface of the MCLs by using an airbrush (Badger Model 150, Franklin Park, IL) to produce markers with suitable contrast for strain calculation (Fig. 1(*a*)). The width and thickness of the MCL cross section were measured

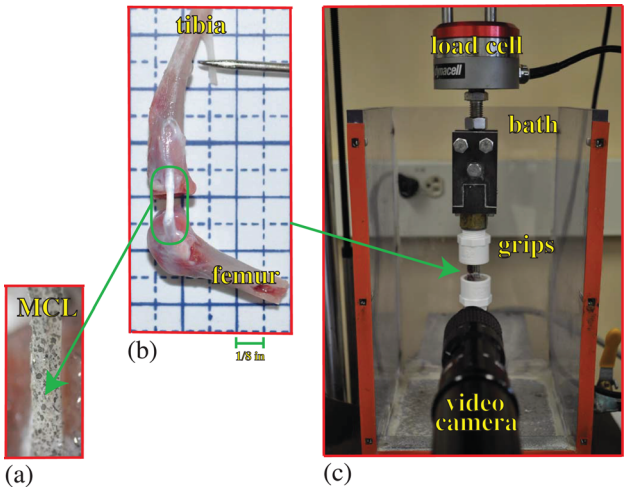

Fig. 1 (*a*) FMTC attached to a frame made of a polyethylene terephthalate sheet at a 70-deg flexion. (*b*) MCL with black ink sprayed on its surface. Two ink markers were selected for strain measurement. (*c*) FMTC mounted on the tensile testing device.

optically using images taken by a digital camera (Nikon D5000) under a dissection stereoscope (Zeiss Stemi 2000 C). Measurements were taken at three different locations and averaged. The cross-sectional areas of the MCLs were calculated by assuming elliptical cross sections.

A strip of fiberglass was attached to the femur of each FMTC using cyanoacrylate glue to reinforce its growth plate, while several notches were created on the tibia to enhance gripping (Fig. 1(*b*)). The tibia and femur in each FMTC were attached to a frame made of a polyethylene terephthalate sheet at a 70-deg flexion to ensure that the MCL was loaded in its anatomic direction [14,15]. The femur, tibia, and plastic frame were potted with bone cement in two hose barbs.

The hose barbs were secured to the mechanical grips of a universal tensile testing machine (Instron ElectroPuls E1000) with vertical mounting. The load cell used had a capacity of 250 N and resolution of 0.001 N. The tibial end of the FMTCs was attached to the upper grip connected to the load cell and the femoral end to the lower grip fixed to a supporting table. Special care was taken to ensure that the FMTCs were aligned along the axis of the load cell. The plastic frames holding the bones were then cut and the FTMCs and grips were immersed in a custom designed bath filled with phosphate buffered saline solution at room temperature (~21 °C) (Fig. 1(*c*)).

During testing, the load data were recorded by the load cell of the tensile testing machine. For each MCL the nominal stress data

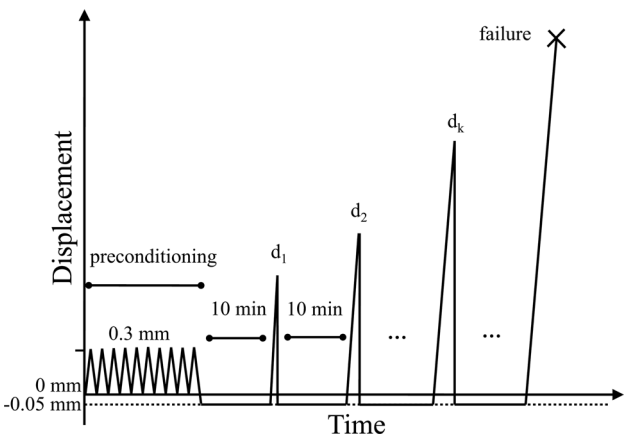

Fig. 2 Schematic of the experimental protocol

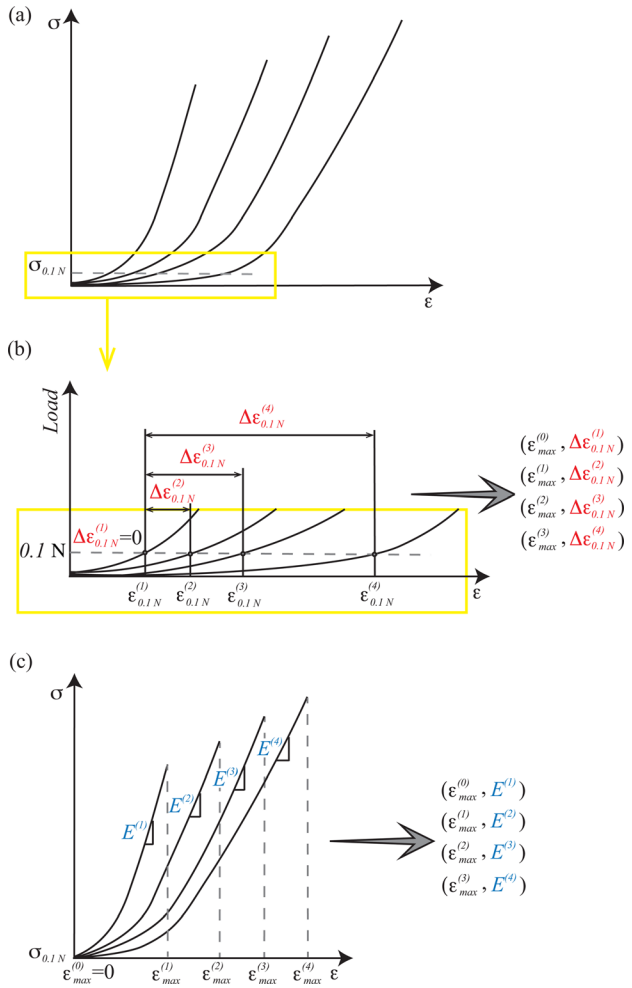

Fig. 3 Schematic of experimentally measured mechanical quantities. (*a*) Stress–strain curves starting from a 0 N load. These are examples of curves obtained by loading one FTMC to four consecutive displacements: $d_1 = 0.45$ mm, $d_2 = 0.65$ mm, $d_3 = 0.85$ mm, $d_4 = 1.05$ mm. Note that $\sigma_{0.1N}$ denotes the stress that corresponds to the 0.1 N load (preload). (*b*) Initial nonlinear load–strain data that are associated with the stress–strain curves shown in (*a*) (left) and measured mechanical quantities (right). Note that the strain is plotted versus the load. $\Delta\varepsilon_{0.1N}^{(k)} = \varepsilon_{0.1N}^{(k)} - \varepsilon_{0.1N}^{(0)}$ for $k = 1, 2, 3, 4$ are shown. Recall that $\varepsilon_{0.1N}^{(k)}$ is the strain at 0.1 N load obtained by loading the FTMC to the displacement d_k and $\varepsilon_{0.1N}^{(0)}$ is the strain at 0.1 N load obtained by loading the FTMC to the first displacement $d_1 = 0.45$ mm. (*c*) Stress–strain curves shown in (*a*) but computed from a 0.1 N preload (left) with measured mechanical quantities (right). For $k = 1, 2, 3, 4$, $E^{(k)}$ defines the tangent modulus of the linear region of the stress–strain curve obtained by loading the FMTC to the displacement d_k and $\varepsilon_{max}^{(k)}$ is the strain that corresponds to the maximum load achieved at d_k.

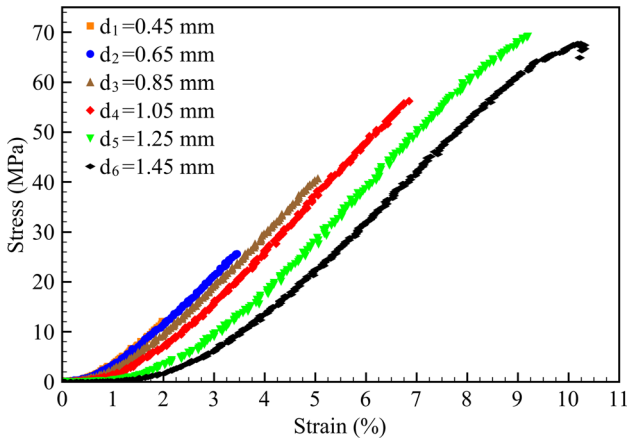

Fig. 4 Typical tensile stress–strain data computed by loading one FMTC to consecutive and increasing displacements d_k for $k = 1, 2, 3, 4, 5, 6$ starting from 0 N load. The values of these displacements are reported in the legend.

were calculated by dividing the load data by its initial cross-sectional area. The displacement of the black ink markers on the surface of the MCL was tracked by a video camera (Photron Ultima APX-RS) at a resolution of 256×1024. Two markers of almost identical shape were selected ~2 mm away from the tibial and femoral MCL insertion sites. Their displacement was measured in pixels by using imaging analysis software (PROANALYST, XCITEX). The Green-Lagrangian strain data in the direction of loading were then computed from the displacement data by assuming that the MCL underwent uniform extension. Thus, the strain was computed as $(L^2 - L_0^2)/2L_0^2$ where L_0 and L are the distances between the markers in the undeformed and deformed configurations, respectively. The visual noise was measured to be approximately 0.07% at 0 N load using the outlier detection method with 1.5 interquartile range.

Displacement-controlled tensile tests were performed on the 30 MCLs. The experimental protocol is schematically presented in Fig. 2. First, each MCL was preconditioned with ten stretching cycles up to 0.3 mm at 1 Hz in order to provide a consistent loading history among all the tested MCLs. This number of cycles was chosen based on previous studies [11]. Then, it was unloaded to −0.05 mm displacement to assure that the initial load state was at 0 N, and allowed to recover for 10 min [11]. After preconditioning and starting from a 0 N load state, the MCL was loaded to a set of increasing displacements, d_k, where $k = 1, 2, 3, \ldots$ and $d_{k+1} - d_k = 0.2$ mm, at a displacement rate of 0.1 mm/s until failure occurred. Between consecutive loads at increasing displacements the MCL was unloaded and allowed to recover from creep for 10 min. Figure 3(*a*) shows an example of the stress–strain curves for one MCL that is loaded to four consecutive displacements starting from a 0 N load state.

The change in elongation of the MCL that occurred when loading the MCL up to the displacement d_k for $k = 1, 2, 3, \ldots$ was quantified by measuring the difference, $\Delta\varepsilon_{0.1N}^{(k)}$, between the strain at 0.1 N load, $\varepsilon_{0.1N}^{(k)}$, obtained by loading the specimen up to the displacement d_k, and the strain at 0.1 N, $\varepsilon_{0.1N}^{(1)}$, obtained by loading the specimen up to the displacement $d_1 = 0.45$ mm (see Fig. 3(*b*) for an example). With this notation $\Delta\varepsilon_{0.1N}^{(1)} = \varepsilon_{0.1N}^{(1)} - \varepsilon_{0.1N}^{(1)} = 0$. Due to noise in the strain measurement, the increase in elongation at 0.1 N was assumed to occur only when $\Delta\varepsilon_{0.1N}^{(k)} > 0.1\%$.

The 0.1 N load was chosen as the preload value in order to eliminate the slack in the MCLs and standardize their initial configuration. The strain in the MCLs was then recalculated with respect to this initial configuration. The strain corresponding to the maximum load achieved with each loading up to the displacement d_k, $\varepsilon_{\max}^{(k)}$, and the tangent modulus of the linear region of the stress–strain curve, $E^{(k)}$, were computed (see Fig. 3(*c*) for an example). The tangent modulus was defined as the slope of the best fit line of linear portion of the stress–strain curve using the method of least squares. The linear portion of the stress–strain curve was determined by drawing a straight line on the stress–strain data. It is important to note that the increase in elongation at preload $\Delta\varepsilon_{0.1N}^{(k)}$ and the decrease in the tangent modulus $E^{(k)}$ of the linear region of the stress–strain curve observed when loading the FMTC up to the displacement d_k were considered to be determined by damage that occurred during the previous loading up to the displacement d_{k-1} and, thus, were associated with

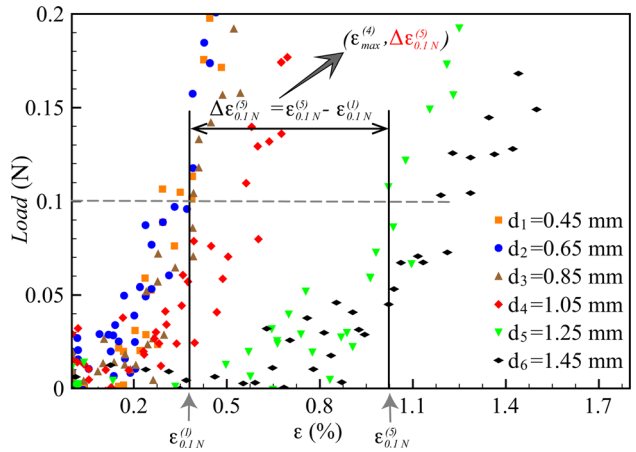

Fig. 5 Load and strain data of the initial nonlinear region for the stress–strain data presented in Fig. 4. The change in elongation at the 0.1 N load (preload) is measured by $\Delta\varepsilon_{0.1N}^{(k)}$ for $k = 1, 2, 3, 4, 5, 6$. This quantity is defined as the difference between the strain at 0.1 N load measured when loading the specimen up to the displacement d_k, $\varepsilon_{0.1N}^{(k)}$, and the strain at 0.1 N load measured when loading the same specimen up to the displacement $d_1 = 0.45$ mm, $\varepsilon_{0.1N}^{(1)}$. For example, $\Delta\varepsilon_{0.1N}^{(5)}$ is computed as shown. This increase in elongation was assumed to be induced by the displacement d_4 (or the strain $\varepsilon_{max}^{(4)}$).

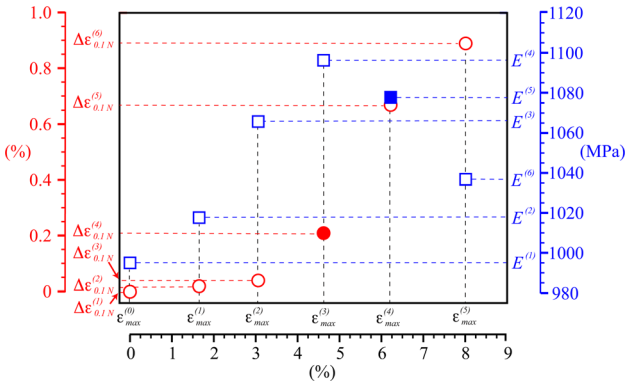

Fig. 7 Change in elongation at preload (0.1 N) (circular symbols) and tangent modulus of the linear region, $E^{(k)}$ (squared symbols), of the stress–strain curve measured when loading one FMTC to the displacement d_k plotted versus the maximum strain $\varepsilon_{max}^{(k-1)}$ obtained when loading the same specimen to the displacement d_{k-1} for $k = 1, 2, 3, 4, 5, 6$. (Note that $\varepsilon_{max}^{(0)} = 0$ and $\Delta\varepsilon_{0.1N}^{(1)} = 0$). The data used to compute these quantities are shown in Figs. 4–and 6. Recall that $\varepsilon_{max}^{(k-1)}$ was assumed to determine $\Delta\varepsilon_{0.1N}^{(k)}$ and $E^{(k)}$. One can note that the elongation at preload starts to increase at the threshold strain $\varepsilon_{max}^{(3)} = 4.62\%$ (filled circular symbol) and the tangent modulus of the linear region of the stress–strain curve starts to decrease at the threshold strain $\varepsilon_{max}^{(4)} = 6.22\%$ (filled squared symbol).

the corresponding strain $\varepsilon_{\max}^{(k-1)}$ (see Figs. 3(*b*) and 3(*c*) for an example).

The stress–strain data collected from 30 FMTCs were analyzed in order to determine threshold strains at which the increase in ligament's elongation at preload and decrease in the tangent modulus of the linear region first occurred. Statistical analysis was performed to determine the difference between the threshold strains indicating the increase in elongation at preload and the decrease in tangent modulus. The Wilcoxon signed-rank test and the JMP software (JMP, Version 9., SAS Institute Inc., Cary, NC, 1989–2010) were used. Statistical significance was established at $P < 0.05$.

3 Results

The typical stress–strain data collected when testing 1 of the 30 FMTCs are shown in Fig. 4. Each of the six stress–strain curves reported in Fig. 4 was obtained by loading the FMTC to consecutive displacements d_k for $k = 1, 2, 3, 4, 5, 6$ starting from a 0 N load reference configuration and using the methods and protocol previously described. It can be clearly seen that, as the displacement d_k increased, the initial nonlinear region of the stress–strain curve becomes more extended, while the tangent modulus of the linear region decreased. In this study, we assumed that these changes in the tensile response of the MCL after consecutive loadings up to different and increasing displacements indicated the initiation and propagation of damage.

For each FMTC, the change in elongation at preload was quantified by measuring $\Delta\varepsilon_{0.1N}^{(k)}$, as defined in Sec. 2, for each loading up to the displacement d_k. It must emphasized again that we assumed that $\Delta\varepsilon_{0.1N}^{(k)}$, which was measured during the loading up to the displacement d_k, was caused by the previous loading up to the displacement d_{k-1} and, thus, was associated with the

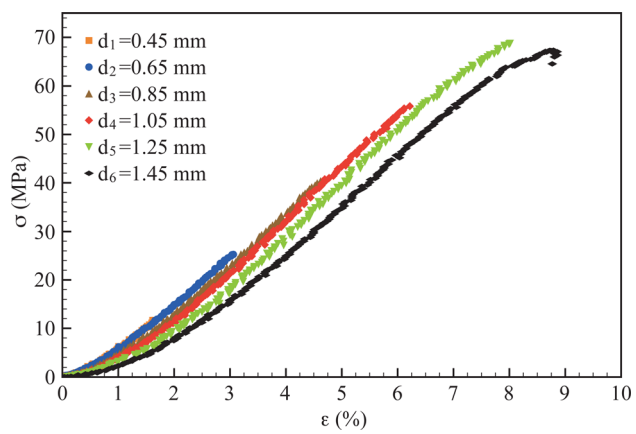

Fig. 6 Stress–strain data for one FTMC (same FTMC used to generate the data in Fig. 4) computed using the 0.1 N load (preload) state as the undeformed configuration for strain measurements

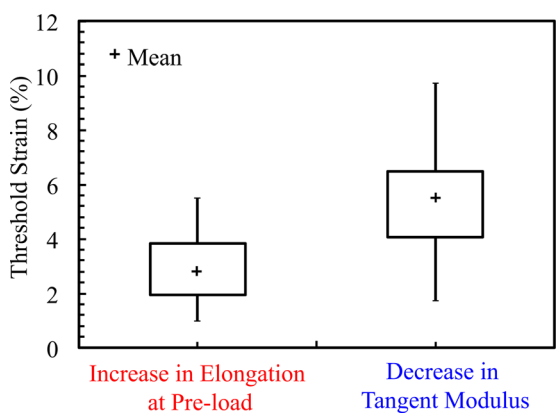

Fig. 8 Box plot of the threshold strains indicating the increase in elongation at preload and decrease in tangent modulus of the linear region of the stress–strain curves for $n = 30$ MCLs

corresponding strain $\varepsilon_{\max}^{(k-1)}$. For the representative stress–strain curve presented in Fig. 4, the load and strain data of the initial nonlinear region that were used to compute $\Delta\varepsilon_{0.1N}^{(k)}$ are presented in Fig. 5 (for example, $\Delta\varepsilon_{0.1N}^{(5)}$ was computed as shown in Fig. 5 and was associated with the strain $\varepsilon_{\max}^{(4)}$). For each loading up to the displacement d_k, the strain corresponding to the maximum load achieved, $\varepsilon_{\max}^{(k)}$, and the tangent modulus of the linear region of the stress–strain curve, $E^{(k)}$, were computed with data determined using the 0.1 N preload as the undeformed configuration. For the data reported in Fig. 4, the stress–strain data computed using the 0.1 N preload state as the undeformed configuration are shown in Fig. 6.

For the selected representative FMTC, $\Delta\varepsilon_{0.1N}^{(k)}$ and $E^{(k)}$ computed from the stress–strain data presented in Figs. 4–6 are plotted versus $\varepsilon_{\max}^{(k-1)}$ for $k = 1, 2, 3, 4, 5, 6$. The results presented in Fig. 7 indicated that the increase in ligament's elongation at preload and the decrease in tangent modulus denoted with a filled circular symbol and a filled squared symbol, respectively, initiated at two very different threshold strains. Specifically, the increase in elongation at preload began at a smaller strain than the decrease in tangent modulus of the linear region: $\Delta\varepsilon_{0.1N}^{(k)}$ started to increase at a 4.62% threshold strain and $E^{(k)}$ started to decrease at a 6.22% threshold strain.

The threshold strains from 30 FMTCs are reported in Fig. 8 in a box plot. The mean value of the strain associated with the elongation at preload was found to be 2.84% (SD = 1.29%), while the mean value of the strain associated with the decrease in tangent modulus of the linear region was determined to be 5.51% (SD = 2.10%). Again, one can observe that the elongation at preload occurred at lower threshold strain than the decrease in tangent modulus of the linear region. Statistical results showed that there was a significant difference between the threshold strain indicating the increase in elongation at preload and the threshold strain indicating the decrease in tangent modulus of the linear region of the stress–strain curve of MCLs ($P < 0.05$).

4 Discussion

In this study, mechanical damage in ligaments was investigated by performing displacement-controlled tensile tests on MCLs excised from rats. The MCLs were stretched to gradually increasing displacements until complete failure occurred. Unrecoverable changes such as the increase in ligament's elongation at preload and decrease in tangent modulus of the linear region of the collected stress–strain curves indicated the initiation and propagation of damage. The threshold strains that produced these changes were computed and their average values were found to be significantly different.

Previous studies on cyclic loading and stretching of parallel-fibered collagenous tissues suggested that the elongation at preload or, equivalently, the increase in tissue's length [1–3,7] and decrease in modulus or stiffness of the linear region of the stress–strain or load–displacement curve [4–6,8] are indicators of tissues' damage. Experiments conducted by stretching these tissues monotonically also produced similar results [9,11]. Thus, our experimental data confirmed the findings of previous studies while also providing strain-based damage thresholds. In our study, the threshold strain for the increase in elongation at preload and decrease in tangent modulus of the linear region of the stress–strain curve were found to be significantly different (Fig. 8). For example, from Figs. 5 and 7, which report the data from one representative MCL, one can clearly note the increase in elongation at preload during the fourth loading up to the displacement d_4 and the decrease in tangent modulus during the sixth loading up to the displacement d_6. In our analysis, we assumed that these changes were the result of damage that occurred during the third and fifth loadings up to the displacement d_3 and d_5, respectively. The strain values that correspond to these displacements, $\varepsilon_{\max}^{(3)} = 4.62\%$ and $\varepsilon_{\max}^{(5)} = 6.22\%$, were found to be significantly different. Our study is the first to report such difference in strain-based damage thresholds. It is possible that different microstructural alterations trigger the different unrecoverable changes that we observed in the elongation at preload and tangent modulus of the linear region of the stress–strain curve of the ligaments.

To our knowledge, there is only one experimental study by Provenzano et al. [11] in which the threshold strain for structural damage was determined by monotonic tensile tests on MCLs isolated from Sprague Dawley rats. In this study, each MCL was subjected to a single stretch, unloaded, allowed to recover from creep, and then stretched to failure. Structural damage was defined by the authors as the change in ligament's length measured at a 0.1 N preload produced by a single stretch. The authors estimated that such damage initiates at 5.14% strain by analyzing the results obtained by testing 25 MCLs using methods described in detail in their manuscript. According to a study by Panjabi et al. [12], single and incremental subfailure stretches are mechanically equivalent, producing the same alterations in the mechanical properties of ligaments. Thus, the protocol we adopted in this study is mechanically equivalent to the protocol used by Provenzano et al. [11]. The decrease in tangent modulus in our study was found to occur at a mean threshold strain (mean = 5.51%, SD = 2.10%) that was comparable with the threshold strain reported by Provenzano et al. [11]. The difference between these strains are, most probably, due to the different methods (e.g., a single stretch versus multiple stretches) used to define and determine the onset of structural damage. For example, in the study by Provenzano et al. [11], the decrease in tangent modulus was quantified together with the increase in ligament's length. By using our methods, the increase in elongation at 0.1 N preload, which is caused by the increase in ligament's length, was found to occur at much lower threshold strain (mean = 2.84%, SD = 1.29%) than the decrease in tangent modulus. For this reason, these threshold strains were not lumped together. We believe that, because our protocol offers more information about the progression of strain-induced damage by applying multiple consecutive stretches to the MCL, it likely provides a more accurate determination of threshold strains [12].

In our experiments, failure of the FMTCs upon stretching occurred mostly at the tibial insertion site. The failure near or at the insertion site is likely determined by the morphology of the FMTCs. In Sprague Dawley rats up to 120 days of age, the MCL inserts into the tibia only through the periosteum with no fibrocartilage zone [16]. Due to the absence of the fibrocartilage zone, the tibial insertion site is the weakest region in the MCLs and, consequently, failure occurs commonly at this site during mechanical testing. Our findings are consistent with recent studies on the effect of cyclic stretching on FMTCs isolated from older Sprague Dawley rats [17], where failure was also reported to occur near the tibial insertion. Given the MCL mode of failure, we cannot exclude the possibility that the damage we measured was the damage of the insertion site of the MCL. The low strain rate (0.1 mm/s) used in our study may have also played a critical role on the failure mode. Indeed, a few studies have suggested that high strain rates are more likely to produce failure at the midsubstance in rat MCLs [18,19].

It is speculated that the increase elongation at preload and the decrease in tangent modulus of the linear region of the stress–strain curve are determined by different microstructural alterations that are induced by strain in ligaments. It is well known that the tensile response of ligaments in the initial nonlinear region is mainly due to the uncrimping of the collagen fibrils [20]. Thus, it is possible that the increase in elongation at preload is caused by the plastic deformation and formation of kinks in collagen fibrils and fibers [1]. The decrease in tangent modulus can be, most probably, attributed to the breakage of groups of collagen fibrils or entire fibers in the ligamentous tissue. Future studies will be conducted by the authors to reveal the microstructural origin of

damage in MCLs by combining mechanical testing with scanning electron microscopy.

Acknowledgment

This material is based upon work supported by the National Science Foundation under Grant No. 0932024.

References

[1] Fung, D. T., Wang, V. M., Laudier, D. M., Shine, J. H., Basta-Pljakic, J., Jepsen, K. J., Schaffler, M. B., and Flatow, E. L., 2009, "Subrupture Tendon Fatigue Damage," J. Orthop. Res., **27**(2), pp. 264–273.

[2] King, G. J. W., Pillon, C. L., and Johnson, J. A., 2000, "Effect of In Vitro Testing Over Extended Periods on the Low-Load Mechanical Behaviour of Dense Connective Tissues," J. Orthop. Res., **18**(4), pp. 678–681.

[3] Pollock, R. G., Wang, V. M., Bucchieri, J. S., Cohen, N. P., Huang, C. Y., Pawluk, R. J., Flatow, E. L., Biqilani, L. U., and Mow, V. C., 2000, "Effects of Repetitive Subfailure Strains on the Mechanical Behavior of the Inferior Glenohumeral Ligament," J. Shoulder Elbow Surg., **9**(5), pp. 427–435.

[4] Schechtman, H., and Bader, D. L., 2002, "Fatigue Damage of Human Tendons," J. Biomech., **35**(3), pp. 347–353.

[5] Thornton, G. M., Schwab, T. D., and Oxland, T. R., 2007, "Fatigue Is More Damaging Than Creep in Ligament Revealed by Modulus Reduction and Residual Strength," Ann. Biomed. Eng., **35**(10), pp. 1713–1721.

[6] Wang, X. T., Ker, R. F., and Alexander, R. M., 1995, "Fatigue Rupture of Wallaby Tail Tendons," J. Exp. Biol., **198**(Pt 3), pp. 847–852.

[7] Wren, T. A. L., Lindsey, D. P., Beaupre, G. S., and Carter, D. R., 2003, "Effects of Creep and Cyclic Loading on the Mechanical Properties and Failure of Human Achilles Tendons," Ann. Biomed. Eng., **31**(6), pp. 710–717.

[8] Zec, M. L., Thistlethwaite, P., Frank, C. B., and Shrive, N. G., 2010, "Characterization of the Fatigue Behavior of the Medial Collateral Ligament Utilizing Traditional and Novel Mechanical Variables for the Assessment of Damage Accumulation," ASME J. Biomech. Eng., **132**(1), p. 011001.

[9] Panjabi, M. M., and Courtney, W., 2001, "High-Speed Subfailure Stretch of Rabbit Anterior Cruciate Ligament: Changes in Elastic, Failure and Viscoelastic Characteristics," Clin. Biomech., **16**(4), pp. 334–340.

[10] Panjabi, M. M., Yoldas, E., Oxland, T. R., and Crisco, J. J., III, 1996, "Subfailure Injury of the Rabbit Anterior Cruciate Ligament," J. Orthop. Res., **14**(2), pp. 216–222.

[11] Provenzano, P. P., Heisey, D., Hayashi, K., Lakes, R., and Vanderby, J. R., 2002, "Subfailure Damage in Ligament: A Structural and Cellular Evaluation," J. Appl. Physiol., **92**(1), pp. 362–371.

[12] Panjabi, M. M., Huang, R. C., and Cholewicki, J., 2000, "Equivalence of Single and Incremental Subfailure Stretches of Rabbit Anterior Cruciate Ligament," J. Orthop. Res., **18**(5), pp. 841–848.

[13] Sengupta, P., 2013, "The Laboratory Rat: Relating Its Age With Human's," Int. J. Prev. Med., **4**(6), pp. 624–630.

[14] Provenzano, P. P., Martinez, D. A., Grindeland, R. E., Dwyer, K. W., Turner, J., Vailas, A. C., and Vanderby, R., Jr., 2003, "Hindlimb Unloading Alters Ligament Healing," J. Appl. Physiol., **94**(1), pp. 314–324.

[15] Thornton, G. M., Shrive, N. G., and Frank, C. B., 2002, "Ligament Creep Recruits Fibres at Low Stresses and Can Lead to Modulus-Reducing Fibre Damage at Higher Creep Stresses: A Study in Rabbit Medial Collateral Ligament Model," J. Orthop. Res., **20**(5), pp. 967–974.

[16] Wei, X., and Messner, K., 1996, "The Postnatal Development of the Insertions of the Medial Collateral Ligament in the Rat Knee," Anat. Embryol., **193**(1), pp. 53–59.

[17] Su, W. R., Chen, H. H., and Luo, Z. P., 2008, "Effect of Cyclic Stretching on the Tensile Properties of Patellar Tendon and Medial Collateral Ligament in Rat," Clin. Biomech., **23**(7), pp. 911–917.

[18] Crowninshield, R. D., and Pope, M., 1976, "The Strength and Failure Characteristics of Rat Medial Collateral Ligaments," J. Trauma Acute Care Surg., **16**(2), pp. 99–105.

[19] Yiannakopoulos, C. K., Kanellopoulos, A. D., Dontas, I. A., Trovas, G., Korres, D. S., and Lyritis, G. P., 2005, "The Symmetry of the Medial Collateral and Anterior Cruciate Ligament Properties. A Biomechanical Study in the Rat Hind Limb," J. Musculoskeletal Neuronal Interact., **5**(2), pp. 170–173.

[20] Viidik, A., and Ekholm, R., 1968, "Light and Electron Microscopic Studies of Collagen Fibers Under Strain," Z. Anat. Entwickl. Gesch., **127**(2), pp. 154–164.